Investigations on supermolecular structure of gel-spun/hot-drawn high-modulus polyethylene fibres

D. Hofmann and E. Schulz
Academy of Sciences of the German Democratic Republic, Institute of Polymer Chemistry 'Erich Correns', Teltow-Seehof, GDR-1530
(Received 27 January 1989; accepted 16 February 1989)

The supermolecular structure of two commercial and two laboratory gel-spun/hot-drawn high-modulus polyethylene (PE) fibres is characterized using wide-angle and small-angle X-ray scattering, electron microscopy and mechanical methods. Two of these samples are composed of smooth microfibrils, while the other two materials reveal a shish kebab morphology. Crystallite sizes, lattice distortions and crystalline orientations are given. For the non-crystalline regions of smooth fibrillar fibres the contents of trapped entanglements, tie and taut-tie molecules are determined. The shish kebab materials are discussed using the crystal continuity model of Ward *et al.* The structural parameters are correlated with the axial Young's modulus of the samples.

(Keywords: polyethylene fibres; gel spinning/hot drawing; supermolecular structure; modulus; wide-angle X-ray scattering)

INTRODUCTION

High-modulus polyethylene (PE) fibres can be prepared via different routes[1–3], but only gel spinning followed by ultra-drawing is used commercially. This is due to the very high rates of fibre production achieved by this procedure.

The main principle is that in the first stage a substantially unoriented gel filament with a very low entanglement density is formed by quenching solutions of low polymer concentration. In the second stage, this entanglement network can be drawn in an oven to very high draw ratios ($\lambda \gg 20$). During this process molecular chains have to be transformed from a folded-chain conformation into a nearly extended-chain conformation. The whole process results in a highly oriented stiff fibre[4–9].

High-modulus PE fibres may exhibit supermolecular structure of different kinds. In most cases a shish kebab morphology is formed. This consists of core microfibrils with nearly extended chains and a number of chain-folded platelets attached to the cores[3,10–13]. There are also fibres that consist mainly of smooth microfibrils with nearly extended molecules, while the content of lamellar platelets is negligible[14–16].

The present paper is mainly concerned with investigations of the supermolecular structure of two smooth microfibril and two shish kebab high-modulus PE fibres (in each case one commercial and one laboratory product). In both cases, besides the structure of the crystalline phase (crystallite sizes, lattice distortions, crystalline orientation), the inner structure of non-crystalline sample regions will be discussed also. For this reason electron microscopy (EM), wide-angle X-ray scattering (WAXS), small-angle X-ray scattering (SAXS) and mechanical investigation techniques were used. The structural parameters obtained will be correlated with the axial Young's modulus of the samples. Furthermore, the results will be compared with the data published recently for some high-modulus PE fibres and for poly(ethylene terephthalate) (PET) samples of relatively high modulus made by multistage zone drawing.

EXPERIMENTAL

Samples

First two commercial high-modulus fibres, Spectra 900 (Allied Sign) and Tekmilon (Mitsui), were investigated. Secondly, two further materials were prepared by us.

Sample 1 was obtained from a 5 wt% solution of Hostalen-GUR (Hoechst $M_w = 1.5 \times 10^6$) in decalin with a small content of antioxidants and aluminium stearate. After spinning in water, the gel filament was treated with ethanol, subsequently dried in air at 373 K and simultaneously drawn to $\lambda_1 = 45$. Then the fibre was zone drawn[17] seven times at different temperatures between 393 and 416 K with increasing load. The resulting total draw ratio was $\lambda = 193$.

Sample 2 was prepared in the same manner but the starting material was a 3 wt% solution of a laboratory product (ZIOC, Rostock) ($M_w \approx 1 \times 10^6$), the drying process was performed at 363 K with $\lambda_1 = 6.8$ and the zone drawing procedure resulted in a total draw ratio $\lambda = 50$.

X-ray investigations

The (1 1 0), (2 0 0), (0 2 0) and (0 0 2) WAXS profiles were measured by symmetrical transmission goniometer scans. Ni-filtered Cu K_α radiation was used. The diffraction profiles were corrected for parasitic scattering, absorption, polarization and Cu K_{α_1,α_2} doublet broadening. The background correction was done according to Vonk[18]. Separation of overlapping reflections was performed with a Pearson VIII function fit program[19–21].

Finally, the WAXS reflection profiles were corrected

0032-3861/89/111964-05$03.00

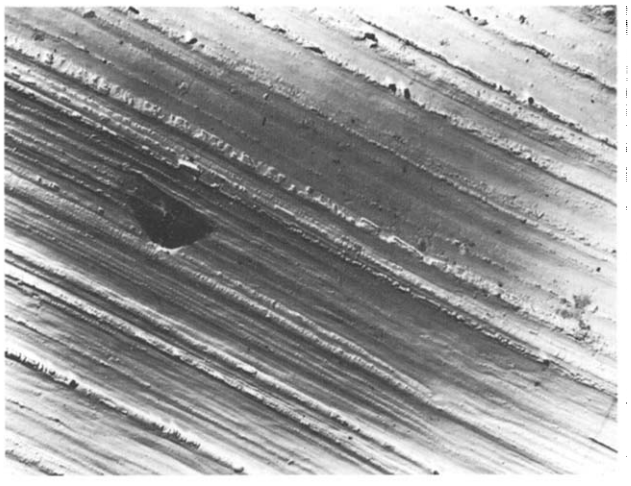

Figure 1 TEM micrograph for sample 1

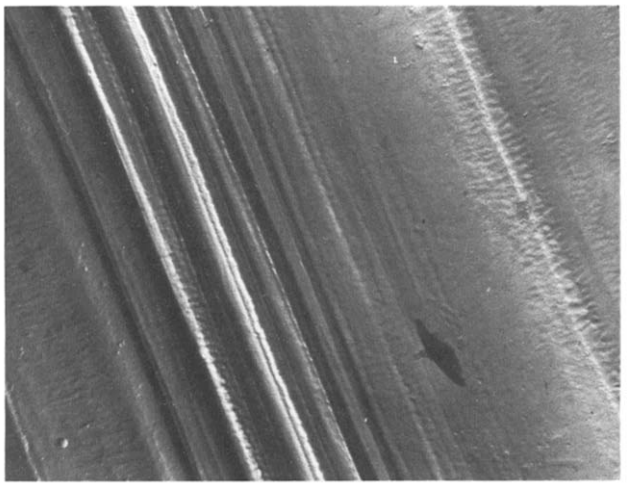

Figure 2 TEM micrograph for Tekmilon sample

for instrumental broadening according to Stokes[22] using an anthracene standard specimen. From the fully corrected and resolved peak profiles the number-average crystallite sizes L_{hkl} and the per cent root-mean-square lattice strain, ε_1, perpendicular to the corresponding scattering lattice planes were obtained by means of a single-line method[23,24].

For samples for which enough material was available, the degree of crystallinity was also determined according to Ruland[25] and Vonk[18], using an approximate isotropic procedure for the WAXS profiles, given in refs 26 and 27.

On the basis of SAXS flat-film photographs the meridional long period L was obtained, if possible. For a nearly smooth fibrillar morphology, L describes the average length of a structural unit element composed of a crystallite and the adjacent non-crystalline region. In this connection the ratio L_{002}/L is the linear degree of order, which is a measure of the crystalline content in the fibre.

Mechanical investigations

Stress–strain curves were recorded at 296 K using an Instron tensile tester (crosshead speed 20 mm min^{-1}). Young's modulus E and the strength σ_{Br} were obtained from these curves. In addition to this the maximum value of thermal shrinkage ($\Delta l/l$) was determined.

Electron microscope investigations

A two-step replica technique was used with Bioden as matrix material and Pt–C thin film as the replica to observe the fibre morphology by TEM.

RESULTS AND DISCUSSION

The EM micrographs reveal that Spectra 900 and sample 1 were mainly composed of smooth microfibrils with only negligible lamellar overgrowth (cf. *Figure 1*), while Tekmilon and sample 2 showed a supermolecular structure of shish kebabs (cf. *Figure 2*). This was confirmed by SAXS photographs. On the one hand, Spectra 900 did not show any meridional intensity maximum, and sample 1 has only a weak meridional peak, which is related to a meridional long period L greater than the meridional crystallite size L_{002}. Tekmilon and sample 2, on the other hand, had distinct meridional reflections (cf. *Figure 3*) and the relation $L < L_{002}$ was met (cf. *Table 1*). (Note that, for Tekmilon, many orders of the meridional SAXS long period were visible even in the WAXS photograph; see *Figure 4*.) The smooth microfibrils of sample 1 were probably due to the higher total degree of drawing ($\lambda = 193$) than in the case of sample 2. This high λ resulted in the unfolding of lamellar crystallized molecular ends, which made these ends intrinsic constituents of the core fibrils (cf. also ref. 11). Under the drawing conditions of sample 2 ($\lambda = 50$), however, many molecular ends of core fibrils will form distinct chain-folded platelets. Furthermore, it should be mentioned that, as shown by the WAXS flat-film photographs, all fibres reveal a very high degree of orientation of crystalline chain axes towards the fibre axis direction (Stein[28] orientation factor f_c near 1; see *Figure 4*) despite the considerable differences in modulus and strength between the materials. This is also true for the intermediate product (after drying/continuous drawing to $\lambda_1 = 45$) of sample 1, while the intermediate product (after drying/continuous drawing to $\lambda_1 = 6.8$) of sample 2 merely shows a medium crystalline orientation. Only orthorhombic material could be detected.

The quantitative results are listed in *Table 1*. For comparison, this table also contains structural and mechanical parameters for a high-modulus PE fibre, obtained in a surface-growth apparatus from a stirred

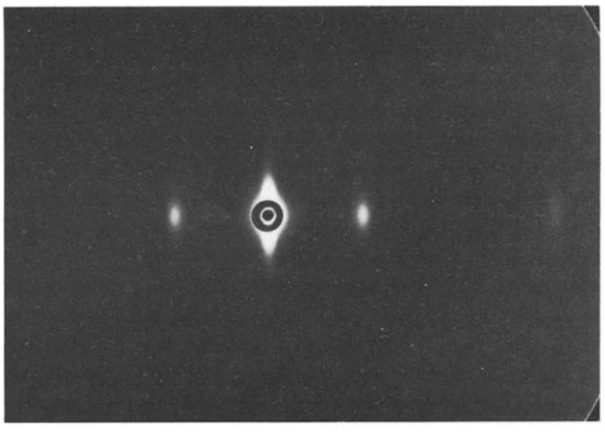

Figure 3 SAXS flat-film photograph for Tekmilon sample

Table 1 Results of structure investigations for the crystalline regions of the high-modulus PE fibres[a]

Sample	Reflection	L_{hkl} (nm)	ε_1 (%)	L (nm)	W_c	σ_{Br} (GPa)	E (GPa)	$\Delta l/l$
Microfibrils								
Spectra 900	(110)	8.9	1.5	(16.0)	0.87	2.3	70	0.88
	(200)	8.6	1.1					
	(020)	11.4	1.0					
	(002)	13.9	1.3					
Sample 1	(110)	13.4	2.5					
	(200)	10.5	1.4	12.3	(0.84)	1.4	36	0.87
	(020)	11.4	1.4					
	(002)	10.3	1.2					
PE4	(110)	7.0	2.1					
	(200)	6.9	1.1	(18.4)	0.90	–	100	0.94
	(002)	16.6	1.6					
Shish kebab fibres								
Tekmilon	(110)	8.3	2.6					
	(200)	7.0	1.4	5.0	0.90–1	2.5	100	0.84
	(020)	7.2	1.4					
	(002)	15.0	1.2					
Sample 2	(110)	9.3	2.4					
	(200)	9.3	1.8	5.1	–	1.7	45	0.90
	(020)	9.5	1.2					
	(002)	12.1	1.3					

[a] L_{hkl} is number-average crystalline size corrected for instrumental broadening and lattice distortions; ε_1 is per cent root-mean-square lattice strain; L is meridional SAXS long period (for smooth fibres, values in pattern are calculated via $L \approx L_{002}/W_c$); W_c is crystallinity (value in pattern calculated via $W_c = L_{002}/L$); σ_{Br} is strength; E is Young's modulus; and $(\Delta l/l)$ is maximum thermal shrinkage. Sample PE4 is cited from refs 26 and 27

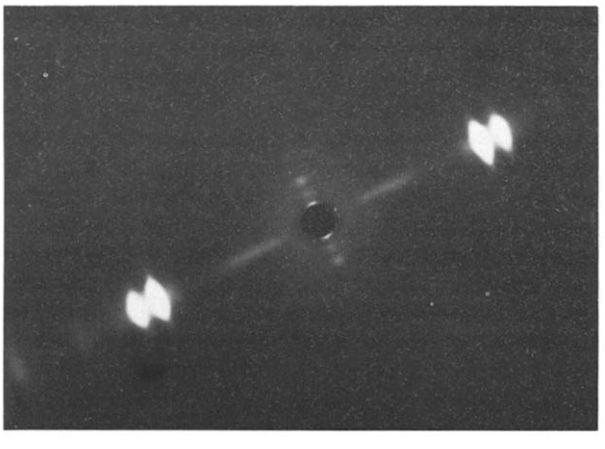

Figure 4 WAXS flat-film photograph for Tekmilon sample

0.5 wt% solution of Hostalen GUR in *p*-xylene at 385 K, and subsequently zone drawn to $\lambda = 1.9$ at 403–413 K. These parameters were first given in other publications[26,27]. (Note that the modulus $E = 100$ GPa is due to the crosshead speed 20 mm min^{-1} used here.)

All materials treated here have crystallite sizes below the few weight-average values H_{hkl} given in the literature for gel-spun PE fibres up to now (not corrected for lattice distortion broadening; e.g. in refs 4 and 29, $H_{200} = 20$ nm, $H_{002} = 70$ nm, $E = 120$ GPa; and in ref. 30, $H_{002} = 26$ nm, $E = 200$ GPa).

But the crystallite sizes and lattice distortion parameters ε_1 for the gel-spun fibres are similar to those previously obtained for a number of surface-grown high-modulus PE fibres[26,27]. Essential correlations between the L_{hkl} and ε_1 values and the axial Young's moduli were not found.

Smooth fibres

Knowledge of orientation, size and perfection of the crystallites, which can be obtained by WAXS, is obviously not sufficient to discuss the correlations between axial elastic modulus under small strain and the supermolecular structure of the PE samples investigated. In this connection the structure of non-crystalline material regions is very important.

Table 2 Results of structure investigations for the non-crystalline regions of the high-modulus PE fibres with smooth microfibrils[a]

Sample	β_1	β_2	i	α
Spectra 900	0.036	0.222	7.8	0.983
Sample 1	0.020	0.114	8.2	0.986
PE4	0.045	0.316	4.7	0.986
120 GPa fibre	0.007	0.380	2.5	0.975

[a] β_1 is relative content of t.t.m. (uniform distribution); β_2 is relative content of t.t.m. (concentration along the boundary of microfibrils); i is average number of trapped entanglements per molecule; and α is relative content of t.m. Results for 120 GPa fibre are calculated from data in refs 4 and 29

It is assumed that for highly oriented structures, composed of nearly smooth fibrils, the fraction of taut (i.e. all-*trans*) tie molecule (t.t.m.) segments between crystallites in one and the same fibril and the linear degree of order (L_{002}/L) are the parameters mainly determining the Young's modulus[31].

Using the same procedure as Peterlin, as described previously for PET samples of higher modulus[26,32] and high-modulus surface-grown PE fibres[26,27], the fraction of t.t.m. can be calculated from the measured E and (L_{002}/L) values. These values are listed in *Table 2* along with β_1, an estimate of t.t.m. assuming a uniform distribution over the cross-section of the non-crystalline regions. The β_2 values were obtained under the assumption that all t.t.m. are located on the outer boundary of the microfibril. The true parameter β is expected to be close to β_1 in the case of surface-grown fibres and in the case of gel-spun/hot-drawn materials. Obviously the lower modulus of sample 1 in comparison to the

commercial product Spectra 900 can be related to the lower content of t.t.m.

Other important structure parameters are the whole average relative content α of intrafibrillar tie molecule (t.m.) segments (taut and not taut) and the average number i of trapped entanglements per molecular chain. According to Kalb, Smook and Pennings[4,29] i can be obtained from measurements of the maximum thermal shrinkage ($\Delta l/l$): assuming for the smooth fibres a molecular weight of $\approx 1 \times 10^6$ (mechanical degradation in the course of spinning roughly considered), the theoretical shrinkage $1-2R_g/l_0$ (l_0 = average contour length of the PE molecules, R_g = radius of gyration of the molecules in the fully relaxed melt) is equal to $1-20.8/M_w^{1/2}=0.979$ for fully extended chains without entanglements. The actual effective extended chain length l_1 in the fibre between entanglements (or backfolds) can then be related to the measured actual shrinkage ($\Delta l/l$):

$$(l_1/l_0)=(1-0.979)/(1-\Delta l/l) \quad (1)$$

Since on average one entanglement reduces the contour length of the molecules by about 20%, the number i of entanglements per molecule may be estimated from[4,28]:

$$(l_1/l_0)=(0.8)^i \quad (2)$$

The i values obtained in this manner are given in *Table 2*. In ref. 29 a semiquantitative estimate is also given for the average relative content α of t.m. based on the number of entanglements i and the two ends of each chain. From this treatment the following approximate formula can be derived[26,27]:

$$\alpha=1-(L/l_0)(2+i) \quad (3)$$

with $l_0 \approx 9070$ nm in the present case and L being the meridional SAXS long period (cf. *Table 1*). The calculated α values are given in *Table 2*. (Note that i could contain backfolds too.) For comparison this table also contains β, i and α parameters for a 120 GPa fibre made by Pennings *et al.*, which were calculated from data given in refs 4 and 29. Obviously the intrafibrillar non-crystalline regions of all investigated samples consist almost completely of tie molecules, but contrary to a statement in ref. 29 only a relatively small number of them are taut. Since only the content of t.t.m. is important for the achieved level of elastic modulus under low strains, no correlation between the parameters i and α on the one hand and the modulus E on the other hand could be found. The same situation is present for surface-grown high-modulus PE fibres[26,27].

Another type of supermolecular structure could be revealed for fibrillar PET samples of modulus higher than for commercial PET fibres and cords[26,32,33]. These materials were obtained via a two- or three-stage drawing procedure from a molten and subsequently quenched non-crystalline precursor material of $M_w=20000$ and showed crystallinities significantly lower (0.25–0.40) than for PE gel-spun/hot-drawn fibres. The amount of intrafibrillar tie molecules was probably not much higher than 10%. These differences to the PE materials investigated here mainly result from the higher chain-end density (lower molecular weight) and the higher entanglement density (precursor obtained from the melt) in the PET samples.

Shish kebab fibres

As already mentioned, sample 2 and the Tekmilon fibres have meridional long periods L lower than the average meridional crystallite size L_{002}. This does not seem to be the case in PE fibres obtained by surface or free growths from stirred solutions[14]. Ward *et al.*, however, found $L_{002}>L$ for some high-modulus PE solid-state extrusion products for which an intercrystalline bridge structure model was proposed[34–37]. We assume that this model may also be applied to the shish kebab fibres investigated by us.

It is then assumed that during the first stages of drawing the original lamellae, which are present after gel spinning, will break into smaller lamellar stacks oriented with their chain axes in the drawing direction. These stacks will then become increasingly linked by crystalline bridges (long crystalline regions of core fibrils) in the further course of drawing. If the crystalline bridges are considered to be randomly distributed over the cross-section of the sample, the following approximate expression given in ref. 34 may be used for the determination of the probability p that a crystalline chain that is fixed in one lamella crosses (as a constituent of a crystallite) an interlamellar region and reaches a neighbouring lamella:

$$p=\frac{L_{002}-L}{L_{002}+L} \quad (4)$$

Probability p also gives the average proportion of area of crystalline material (core fibrils of high crystallinity) in an interlamellar layer. Application of equation (4) gives $p=0.50$ for Tekmilon and $p=0.41$ for sample 2. This means that for these samples the difference in p (note that typical p values[34,36] for high-modulus PE extrudates are 0.25–0.4) is only about 20%, while the axial modulus of Tekmilon is about twice the modulus of sample 2. Therefore it may be concluded that the axial modulus of the studied shish kebab fibres depends not only on the crystal continuity parameter p but also on the inner structure (content of t.t.m., crystallinity) of core fibrils.

In the crystal continuity model the meridional long period L is approximately the mean distance between the centres of neighbouring lamellae. This distance is composed of a mean crystalline intralamellar portion L_c and a mean non-crystalline interlamellar portion L_a. Since the crystallinity of gel-spun/hot-drawn PE fibres is usually very high, the L_a/L_c ratio will be very small. This means that, for $L=5$ nm, $p=0.5$ and $W_c=0.95$, the average thickness of interlamellar layers is about 0.5 nm or less. From the volume of such a layer, 50% for Tekmilon and 41% for sample 2 is occupied by intercrystalline bridges (core fibrils), while the remaining part of a layer mainly contains regular backfolds and chain ends. Because of the many visible orders of the meridional SAXS reflection in the case of Tekmilon (cf. *Figure 4*), the distribution of the axial dimensions of lamellar and interlamellar layers has to be very sharp for this material. The length of a crystallite in the core fibril of this sample is about 25 nm = $((L_{002}-(1-p).4.5\text{ nm})/p)$.

CONCLUSIONS

High-modulus PE fibres of rather different supermolecular structures may result from gel-spinning/hot-drawing procedures. Under high degrees of drawing, often smooth fibrillar structures occur, which are mainly composed of

nearly extended-chain core fibrils. The inner structure (crystallite sizes, lattice distortions) of their crystalline phase does not correlate with the achieved elastic modulus and tenacity levels. Furthermore a high degree of crystalline orientation is a necessary but not a sufficient condition for obtaining high-modulus specimens.

These facts confirm the importance of the structure of the non-crystalline intrafibrillar regions. It can be shown that nearly all ($\approx$98%) molecular segments in these regions are intercrystalline tie molecule segments but only a smaller portion of them is taut (cf. *Table 2*). The axial Young's modulus of smooth fibrillar samples is a function of the content of these taut tie molecule segments and the crystallinity of the samples.

Especially under lower degrees of drawing, high-modulus fibres with a considerable shish kebab morphology may be obtained. (Note that the Young's modulus obviously depends not only on the total drawing ratio but also on the special regime of drawing; cf. preparation conditions of samples 1 and 2.) In this case both nearly extended-chain core fibrils and lamellar material portions are present. For the shish kebab fibres investigated here, the crystal continuity model of Ward *et al.* may be adopted. This means that the samples are composed of crystalline fold lamellae linked by crystalline bridges (crystalline regions of core fibrils). The content p of crystalline bridges is about 40–50%. The average distance L between the centres of neighbouring lamellae is 5 nm including an interlamellar layer distance $L_a \approx 0.5$ nm.

The axial Young's modulus then depends on both the crystal continuity parameter p and the inner structure of core fibrils (content of t.t.m., crystallinity).

REFERENCES

1 'Ultra High Modulus Polymers' (Eds. A. Ciferri and I. M. Ward), Applied Science, London, 1979
2 Black, W. B. *Annu. Rev. Mater. Sci.* 1980, **10**, 311
3 Barham, P. J. and Keller, A. *J. Mater. Sci.* 1985, **20**, 2281
4 Kalb, B. and Pennings, A. J. *J. Mater. Sci.* 1980, **15**, 2284
5 Smith, P. and Lemstra, P. J. *Polymer* 1980, **21**, 1341
6 Smith, P., Lemstra, P. J., Pijpers, J. P. L. and Kiel, A. M. *Colloid Polym. Sci.* 1981, **259**, 1070
7 Pennings, A. J., van der Hooft, R. J., Postema, A. R., Hoogsteen, W. and ten Brinke, G. *Polym. Bull.* 1986, **16**, 167
8 Lemstra, P. J., Bastiaansen, C. W. M. and Meijer, E. H. *Angew. Makromol. Chem.* 1986, **145/146**, 343
9 Lemstra, P. J., van Aerle, N. A. J. M. and Bastiaansen, C. W. M. *Polym. J.* 1987, **19**, 85
10 Pennings, A. J. *J. Polym. Sci., Polym. Symp.* 1977, **58**, 55
11 van Hutten, P. F. and Pennings, A. J. *Makromol. Chem., Rapid Commun.* 1980, **1**, 477
12 Hill, M. J., Barham, P. J. and Keller, A. *Colloid Polym. Sci.* 1980, **258**, 1023
13 Hill, M. J., Barham, P. J. and Keller, A. *Colloid Polym. Sci.* 1983, **261**, 721
14 Zwijenburg, A., van Hutten, P. F., Pennings, A. J. and Chanzy, H. D. *Colloid Polym. Sci.* 1978, **256**, 729
15 Smook, J., Torfs, J. C., van Hutten, P. F. and Pennings, A. J. *Polym. Bull.* 1980, **2**, 293
16 van Hutten, P. F., Koning, C.E. and Pennings, A.J. *Makromol. Chem., Rapid Commun.* 1983, **4**, 605
17 Schulz, E., Bauer, A. and Hofmann, D. *Acta Polym.* 1988, **39**, 181
18 Vonk, C. G. *J. Appl. Crystallogr.* 1973, **6**, 148
19 Heuvel, H. M., Huisman, R. and Lind, K. C. J. B. *J. Polym. Sci., Polym. Phys. Edn.* 1976, **14**, 921
20 Fink, H.-P., Fanter, D. and Philipp, B. *Acta Polym.* 1985, **36**, 1
21 Walenta, E., Janke, A., Hofmann, D., Fanter, D. and Geiss, D. *Acta Polym.* 1986, **37**, 557
22 Stokes, A. R. *Proc. Phys. Soc. Lond. (A)* 1948, **61**, 382
23 Hofmann, D. and Walenta, E. *Polymer* 1987, **28**, 1271
24 Hofmann, D., Fink, H.-P. and Philipp, B. *Polymer* 1989, **30**, 237
25 Ruland, W. *Acta Crystallogr.* 1961, **14**, 1180
26 Hofmann, D. Dissertation A, Teltow, 1987
27 Walenta, E., Hofmann, D., Zenke, D. and Geiss, D. *Acta Polym.* 1989, **40**, 309
28 Stein, R. S. *J. Polym. Sci.* 1958, **31**, 327
29 Smook, J. and Pennings, A. J. *Colloid Polym. Sci.* 1984, **262**, 712
30 Sawatari, C. and Matsuo, M. *Colloid Polym. Sci.* 1985, **263**, 783
31 Peterlin, A. 'Ultra High Modulus Polymers' (Eds. A. Ciferri and I. M. Ward), Applied Science, London, 1979
32 Hofmann, D., Göschel, U., Walenta, E., Geiss, D. and Philipp, B. *Polymer* 1989, **30**, 243
33 Geiss, D. and Hofmann, D. *Prog. Polym. Sci.* in press
34 Gibson, A. G., Davis, G. R. and Ward, I. M. *Polymer* 1978, **19**, 683
35 Clements, J., Jakeways, R. and Ward, I. M. *Polymer* 1978, **19**, 639
36 Capaccio, G., Gibson, A. G. and Ward, I. M. 'Ultra High Modulus Polymers' (Eds. A. Ciferri and I. M. Ward), Applied Science, London, 1979
37 Clements, J. and Ward, I. M. *Polymer* 1983, **24**, 27